Side-Chain Liquid-Crystalline Polymers from the Alternating Copolymerization of Maleic Anhydride and 1-Olefins Carrying Biphenyl Mesogens

René P. Nieuwhof, Antonius T. M. Marcelis, and Ernst J. R. Sudhölter*

Laboratory of Organic Chemistry, Department of Biomolecular Sciences, Wageningen University and Research Center, Dreijenplein 8, 6703 HB Wageningen, The Netherlands

Stephen J. Picken

Akzo Nobel Central Research, Velperweg 76, 6800 SM Arnhem, The Netherlands

Wim H. de Jeu

FOM Institute for Atomic and Molecular Physics, Kruislaan 407, 1098 SJ Amsterdam, The Netherlands

Received September 2, 1998; Revised Manuscript Received November 23, 1998

ABSTRACT: Side-chain liquid-crystalline copolymers (SCLCPs) were synthesized from the alternating copolymerization of maleic anhydride with mesogenic 1-olefins. These SCLCPs showed high glass transition temperatures and highly ordered smectic mesophases. The mesophase width increased with spacer length. The terminal alkyl group length determined the degree of order in the hexatic mesophase that was present just above the glass transition temperature. A terminal methoxy group induced a hexatic smectic B mesophase, intermediate terminal alkyl groups induced a smectic E mesophase, and long terminal alkyl groups induced a crystal smectic B mesophase. If the spacer was shorter than the terminal alkyl group, an interdigitated smectic A mesophase was found in which the terminal alkyl groups overlap. A strong correlation was found between the glass transition temperature and the temperature at which the hexagonal or orthorhombic ordered mesophase disappears. Introduction of an ester linkage between the spacer and biphenyl mesogen or replacing the terminal alkoxy group by a cyano terminal group induced a lowering of transition temperatures and a lower degree of order in the mesophase.

1. Introduction

Since the introduction of side-chain liquid-crystalline polymers (SCLCPs) much effort has been put in studying the effect of molecular architecture on their liquid-crystalline properties.[1−4] The most common structural variables are spacer length, type of mesogen and length and type of the mesogenic terminal group. The properties of SCLCPs are also strongly influenced by the nature of polymer backbone.[2,3,5,6] In the past, attention has been mainly focused on homopolymers such as poly(acrylate)s,[4] poly(siloxane)s,[7] poly(phosphazene)s,[8] and poly(styrene)s.[9]

By copolymerization of two different monomers, polymers can be obtained in which the phase transitions and properties can be tuned to desired levels. A well-defined type of copolymerization is the alternating copolymerization in which the two monomers enter into the copolymer in equimolar amounts and in an alternating arrangement along the copolymer chain. Only few examples of alternating SCLCPs are known: (i) polymers consisting of mesogenic vinyl ethers and mesogenic fumarates[10] and (ii) polymers consisting of mesogenic vinyl ethers and maleic anhydride (MA).[11,12]

Because of the extremely low tendency of MA to homopolymerize, MA forms alternating polymers with olefins that also have a low tendency to homopolymerize.[13,14] Furthermore, a recent study describes the alternating polymerization of maleic acid derivatives with a variety of donor monomers.[15] UV-spectroscopy and Monte Carlo simulations showed that the alternating copolymerization arises from the strong interactions between electron-poor and electron-rich monomers which result in donor−acceptor combinations that subsequently homopolymerize.

Thery et al.[21] found that anhydride moieties in polymers are chemically reactive toward oxidized surfaces and form strong bonds of the carboxylate type. During heat treatment, the anhydride moieties of the polymers migrate to the metal oxide surface. Van der Wielen et al.[16,17] found that heat treatment of spin-coated films of some of the described SCLCPs on silica surfaces results in structures with an almost perfect smectic periodicity.

The presence of anhydride moieties results in low backbone flexibility and consequently a high glass transition temperature (T_g). This high T_g combined with the adhesive properties of MA moieties to metals,[18−21] may be beneficial to application of the present SCLCPs in coatings and corrosion protection,[19,22,23] in which SCLCPs should retain their mechanical stability up to high temperatures.

In this study we describe the synthesis and phase behavior of alternating copolymers of MA with 1-olefins containing alkoxybiphenyl mesogens. The influence of spacer length and terminal alkyl group length on the transition temperatures is studied. Alkoxybiphenyl mesogens were used because they are easily available and their terminal alkyl group length can easily be changed. For comparison a compound with a cyanobiphenyl mesogen was also included in this study. The SCLCPs have been characterized by gel permeation chromatography, ^{1}H NMR, ^{13}C NMR, polarizing optical micros-

10.1021/ma981393d CCC: $18.00
Published on Web 02/17/1999

Table 1. Yields (%) and Melting Temperatures (°C) of 4-Hydroxy-4′-alkoxybiphenyl (2-*p*)

p	yields	melting temperature
0	65	182
2	67	174
3	43	169
5	63	156
7	74	153
8	47	150

copy, differential scanning calorimetry and wide-angle X-ray diffraction.

2. Experimental Part

Materials. The tetrahydrofuran (THF) which was used for the polymerization reactions was purified by distillation over sodium under nitrogen atmosphere. Maleic anhydride was sublimated before use and azoisobutyronitrile (AIBN) was recrystallized twice from methanol. Other reagents used for syntheses were commercially available and used without further purification. 1-Alkylene-ω-tosylate,[24] 4-hydroxy-4′-methoxybiphenyl[25] (**2-0**), 4-methoxy-4′-undec-10-enoylbiphenyl[26] (**4**), and 4-cyano-4′-undec-10-enyloxybiphenyl[27] (**5**) were synthesized according to literature procedures.

Equipment. Gel permeation chromatography (GPC) measurements were carried out using a series of four microstyragel columns with pore sizes of respectively 10^5, 10^4, 10^3, and 10^6 Å (Waters) with THF containing 5 wt % acetic acid as eluent. A dual detection system consisting of a differential refractometer (Waters model 410) and a differential viscometer (Viscotek model H502) was used. A calibration line was made with this setup, using narrow polystyrene reference standards in THF, and the molar mass (g/mol) of the synthesized polymers was determined referring to this calibration line. Thermal transitions were monitored with a Perkin-Elmer DSC-7. Scan rates of 10 K/min were used in the differential scanning calorimetry (DSC) experiments with sample masses of 5−15 mg. Transition temperatures were taken from the second heating cycle. Polarizing optical microscopy (POM) was performed on an Olympus BH-2 microscope equipped with a Mettler FP82HT hot stage and an FP80HT temperature controller. X-ray diffraction measurements were performed on a Siemens D5000 reflection diffractometer with a HTK oven and Cu Kα radiation. ^{1}H NMR spectra were recorded on a Bruker AC200 spectrometer at 200 MHz. FTIR spectra were recorded on a BioRad FTS-7 spectrometer.

Synthesis. 4-Hydroxy-4′-alkoxybiphenyl (2-*p*). All compounds were synthesized according to the same procedure, an example is given for $p = 7$:

1-Bromooctane (3.75 g, 19.4 mmol) was added to a stirred suspension of compound **1** (10.0 g, 54.0 mmol), potassium hydroxide (1.15 g, 20.5 mmol), and a catalytic amount of potassium iodide in ethanol (105 mL) and water (6.5 mL). After stirring at reflux temperature under nitrogen atmosphere for 24 h, the reaction mixture was concentrated by evaporation of the solvent, the residue was dissolved in ethyl acetate and washed with water. After being dried with magnesium sulfate, the solution was evaporated to dryness. The product was purified by silica gel chromatography with a mixture of 1.8 vol % methanol in dichloromethane as eluent. Recrystallization from ethanol yielded colorless crystals (4.26 g, 14.3 mmol, 74%).

^{1}H NMR (acetone-d_6): $\delta = 7.45$ (2d, biphenyl, 4H); 6.91 (2d, biphenyl, 4H); 4.00 (t, $-CH_2O$, 2H); 1.77 (quintet, $-CH_2CH_2O$, 2H); 1.18−1.51 (m, $-CH_2-$, 10H); 0.87 (t, $-CH_3$, 3H).

Yields and melting temperatures for the homologous compounds are given in Table 1.

4-Alkoxy-4′-alk-ω-enyloxybiphenyl (3-*m*,*p*). All compounds were synthesized according to the same procedure, an example is given for $m = 9$ and $p = 0$:

1-Undecene-11-tosylate (or the corresponding 11-bromo-1-undecene) (7.5 g, 23.1 mmol) was added to a stirred suspension of 4-hydroxy-4′-methoxybiphenyl (4.4 g, 22.0 mmol), potassium carbonate (4.76 g, 33.0 mmol) and a catalytic amount of potassium iodide in 2-butanone (105 mL). After stirring at reflux temperature under nitrogen atmosphere for 24 h, the reaction mixture was concentrated by evaporation of the solvent, dissolved in dichloromethane and washed subsequently with water, 10% NaOH and water. After being dried with magnesium sulfate, the solution was evaporated to dryness. Recrystallization from petroleum ether 60/80 yielded colorless crystals (7.25 g, 20.6 mmol, 94%).

^{1}H NMR ($CDCl_3$): $\delta = 7.45$ (2d, biphenyl, 4H); 6.93 (2d, biphenyl, 4H); 5.81 (m, $=CH-$, 1H); 4.91 (2d, $CH_2=$, 2H); 3.97 (t, $-CH_2O$, 2H); 3.83 (s, CH_3OAr-, 3H); 2.03 (q, $=CHCH_2$, 2H); 1.79 (quintet, $-CH_2CH_2O$, 2H); 1.21−1.54 (m, $-CH_2-$, 12H).

Yields and transition temperatures for the homologous compounds are given in Table 2. The yield of monomer **3-2,0** was 20%, because in that case elimination of HBr during etherification is an important side reaction.

Table 2. Yields (%) and Phase Transition Temperatures (°C) of Monomers 3-*m*,*p*, 4, and 5[a]

monomer	yield	transition temperatures
3-2,0	20	K 121 I
3-3,0	86	K 122 I
3-4,0	89	K 113 I
3-6,0	72	K 106 I
3-8,0	79	K 105 I
3-9,0	94	K 107 I
3-9,2	90	K 107 I
3-9,3	88	K 108 I
3-9,5	91	K 101 (40) S_A 104 (27) I
3-9,7	92	K 98.9 (29) S_X 99.4 (10) S_C 101 (0.25) S_A 104 (30) I
3-9,8	56	K 98.2 (89) S_A 99.0 (17) I
3-3,8	93	K 115 (18) S_A 116 (39) I
3-4,7	89	K 110 I
3-6,5	82	K 111 I
3-8,3	93	K 109 I
4	79	K 74.8 (358) N 78.1 (2.2) I
5[27]	86	K 57.6 (106) S_A 74.1 (1.5) N 75.1 (3.3) I

[a] In case of liquid crystalline behavior the entropy changes (J/mol K) at phase transitions and the mesophase types are given. K = crystalline, $S_{A,C}$ = different smectic phases, S_X = not identified, N = nematic, I = isotropic phase.

Polymerization of Maleic Anhydride and 3-*m*,*p*, 4, or 5 (6-*m*,*p*; 7 and 8). All copolymers were synthesized according to a modified literature procedure,[28] an example is given for $m = 9$ and $p = 0$:

Maleic anhydride (0.73 g, 7.4 mmol), 4-methoxy-4′-undec-10-enyloxybiphenyl (2.5 g, 7.1 mmol), and AIBN (12.8 mg, 0.075 mmol) were dissolved in freshly distilled THF (3 mL), and the mixture was placed in a sealable glass pressure vessel. A vacuum line capable of <2 kPa was used to degas the mixture by three or four freeze−thaw cycles, and the vessel was put under argon at 1.1×10^5 Pa and placed in an oil bath of 60 °C. After 14 days the vessel was cooled, the pressure was released and THF was added. The solution was added to cold methanol (10 volumes) to precipitate the polymer. The latter was collected and repeatedly precipitated from THF into petroleum ether 40/60 (10 volumes) to remove unreacted monomer (in some cases diethyl ether was used to precipate the polymer). A white powder (2.35 g, 74%) was obtained after filtration.

^{13}C NMR signals (solution in acetone-d_6) of the polymer backbone were in excellent agreement with that reported for a highly alternating propene−maleic anhydride copolymer.[29]

Anal. Calcd for polymer **8**, calculated for a 1:1 copolymer: C, 75.5; H, 7.01; N, 3.14. Found: C, 75.3; H, 7.28; N, 2.99.

3. Results and Discussion

3.1. Monomers. The synthesis of monomers **3-*m*,*p*** and the structure of monomers **4** and **5** are depicted in Scheme 1. All monomers were obtained in satisfactory yields and high purity. The observed ^{1}H NMR signals agree well with the chemical structure.

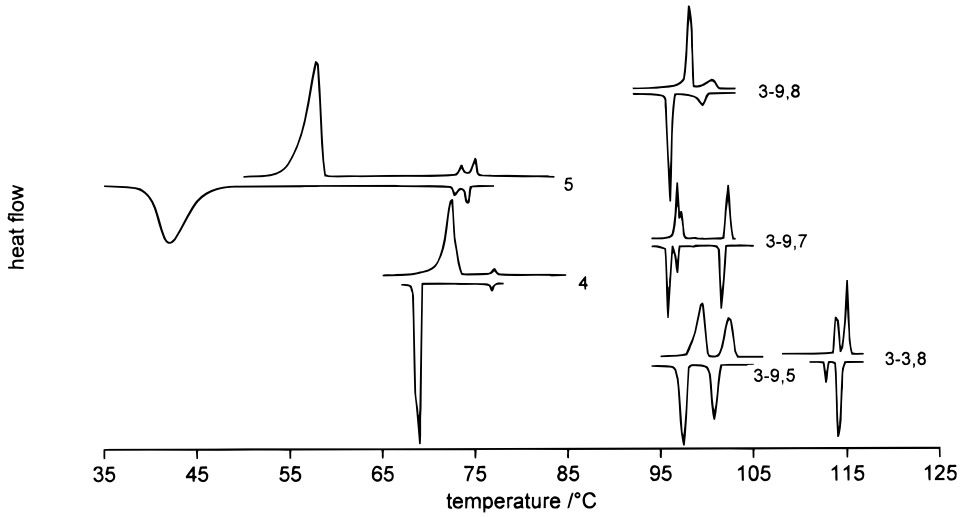

Figure 1. DSC thermograms of monomers **3-3**,**8**, **3-9**,**5**, **3-9**,**7**, **3-9**,**8**, **4**, and **5**. For all compounds the second heating and cooling traces are given.

Scheme 1. Synthesis of Monomers 3-*m*,*p*, 4, and 5

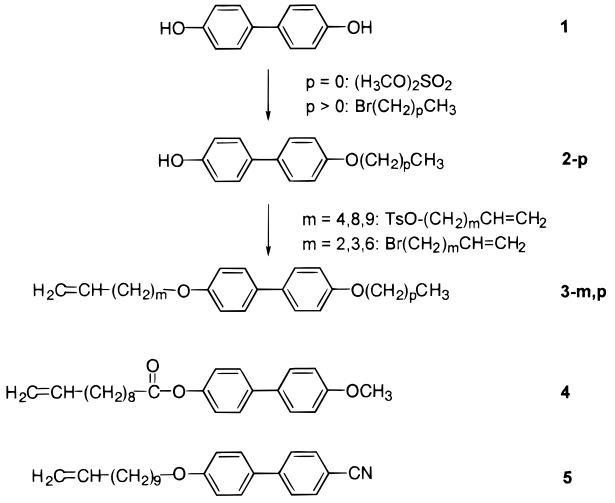

Scheme 2. Synthesis of Polymers 6-*m*,*p*, 7, and 8

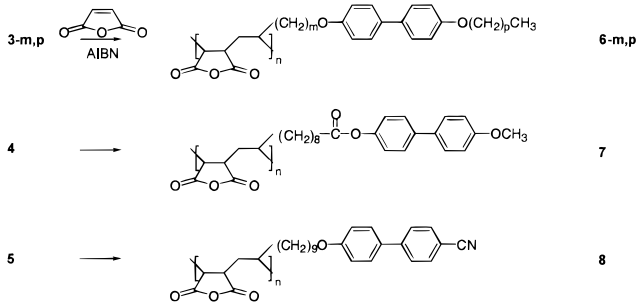

The DSC thermograms in Figure 1 show that monomers **3-3**,**8**, **3-9**,**5**, **3-9**,**7**, **3-9**,**8**, **4**, and **5** exhibit liquid-crystalline behavior and that their phase transitions are reversible. The transition temperatures and corresponding entropy changes, which were determined from DSC traces, are summarized in Table 2. The mesophases were characterized based on the textures observed with polarizing optical microscopy (POM). Transition temperatures observed with POM were in good agreement with those found with DSC.

All liquid-crystalline monomers showed common smectic and/or nematic mesophases, however, monomer **3-9**,**7** exhibited an additional mesophase (S_X) after melting at 98.9 °C. The X-ray diffraction pattern of this mesophase displayed reflections up to the fifth order corresponding to *d* spacings of 31.1, 16.2, 10.0, 7.5, and 6.0 Å. The length of the molecule, which is 34 Å, and the amount of reflections indicate that a regularly layered smectic mesophase was formed without interdigitation. However, from the absence of a sharp reflection corresponding to a *d* spacing of about 4.4 Å, it can be concluded that no order was present within these layers. The S_X mesophase transformed into a smectic C (S_C) mesophase at 99.4 °C and a smectic A (S_A) mesophase at 101.3 °C. In the DSC thermogram, the S_C-S_A transition is not represented by an endothermic peak but an exothermic shift in baseline upon heating. Monomer **5** has been described before[27] and the transition temperatures were in good agreement with those found in the literature.

3.2. Polymer Synthesis. Polymers **6-*m*,*p***, **7**, and **8** were synthesized according to Scheme 2. Before further characterization was performed, polymers were dried in vacuo over P_2O_5 at 100 °C until FTIR showed that the carboxylic acid groups, which were formed to a small degree due to hydrolysis during workup and storage, were ring closed again to anhydride moieties by a dehydration reaction.[12] This process was characterized by the disappearance of the C═O stretching band characteristic for a carboxyl group at 1733 cm^{-1} and the appearance of the symmetric and antisymmetric stretching bands at 1861 and 1780 cm^{-1} typical for an anhydride. ^1H NMR signals corresponded to the expected chemical structures. Broadening of the signals and disappearance of the vinyl signals indicated polymer formation.

It is well-known that (i) MA has an extremely low tendency, if any, to homopolymerize in a radical polymerization[13] and (ii) MA copolymerizes with unactivated 1-alkenes to give highly alternating 1:1 copolymers.[14] Elemental analysis of polymer **8** was consistent with this. Furthermore, the ^{13}C NMR signals of the polymer backbone of polymer **6-9**,**0** were in excellent agreement with that reported for a highly alternating propene–MA copolymer.[29]

The molecular weights of the polymers were determined by GPC and are listed in Table 3. Interactions between the polymer and the packing material of the GPC column were avoided using THF with 5% acetic

Table 3. Number-Average Molecular Weights (M_n), Weight-Average Molecular Weights (M_w), Polydispersity Indices (PDI), Degrees of Polymerization (DP) As Determined by GPC, and Yields (%) of Polymers 6-*m*,*p*, 7, and 8

polymer	$10^{-3}M_n$	$10^{-3}M_w$	PDI	DP	yield
6-2,0	2.01	2.67	1.32	11	20
6-3,0	2.81	5.26	1.87	15	54
6-4,0	3.99	6.54	1.64	21	90
6-6,0	3.27	5.66	1.73	16	76
6-8,0	3.74	5.98	1.60	17	57
6-9,0[a]	3.37	5.32	1.58	15	74
6-9,0[b]	4.05	5.43	1.34	18	65
6-9,2	4.44	6.51	1.47	19	59
6-9,3	4.48	6.34	1.42	18	57
6-9,5	3.43	4.86	1.42	13	60
6-9,7	4.11	5.89	1.43	15	43
6-9,8	3.17	4.49	1.42	11	49
6-3,8	3.02	4.48	1.48	13	63
6-4,7	3.34	4.81	1.44	14	62
6-6,5	4.29	6.96	1.62	18	58
6-8,3	5.55	8.10	1.46	23	61
7	5.09	7.82	1.54	22	59
8	5.89	8.42	1.43	26	60

[a] First batch. [b] Second batch.

Table 4. Phase Transition Temperatures in °C (Corresponding Heat Capacity or Entropy changes in J/mol K) As Determined by DSC and Phase Types of Polymers 6-*m*,*p*, 7, and 8[a]

polymer	transition temperatures
6-2,0	G 112 (117) I
6-3,0	G_{Bhex} 146 (123) S_{Ad} 170 (7.4) I
6-4,0	G_{Bhex} 120 (−) S_{Bhex} 128 (7.1) S_{Ad} 136 (10) I
6-6,0	G_{Bhex} 129 (112) S_{Bhex} 140 (5.6) S_{Ad} 161 (8.1) I
6-8,0	G_{Bhex} 103 (61) S_{Bhex} 117 (5.7) S_{Ad} 156 (13) I
6-9,0[b]	G_{Bhex} 99 (81) S_{Bhex} 112 (3.7) S_{Ad} 164 (13) I
6-9,0[c]	G_{Bhex} 101 (104) S_{Bhex} 111 (3.3) S_{Ad} 165 (16) I
6-9,2	G_E 142 (99) S_E 156 (14) S_{Ad} 177 (9.0) I
6-9,3	G_E 143 (124) S_E 158 (19) S_{Ad} 181 (17) I
6-9,5	G_E 133 (266) S_E 146 (21) S_{Ad} 165 (14) I
6-9,7	G_{Bcryst} 129 (119) S_{Bcryst} 139 (12) S_{Ad} 160 (21) I
6-9,8	G_{Bcryst} 118 (113) S_{Bcryst} 127 (11) S_{Ad} 144 (12) S_{Adt} 151 (7.7) I
6-3,8	G 129 (115) S_{Adt} 208 (3.7) I
6-4,7	G 117 (87) S_{Adt} 187 (5.2) I
6-6,5	G_{Bhex} 118 (91) $S_{Ad/Adt}$ 163 (7.8) I
6-8,3	G_E 147 (158) S_E 159 (17) S_{Ad} 181 (16) I
7	G 86 (57) S_{Ad} 122 (7.3) I
8	G 70 (26) N 99 (3.9) I

[a] I = isotropic phase; $S_{Ad,Adt}$ = different smectic A phases; S_{Bhex} = hexatic smectic B; S_{Bcryst} = crystal smectic B; S_E = smectic E; G_X = glass phase, in which X is the hexagonally ordered mesophase. [b] First batch. [c] Second batch.

acid as an eluent.[30] The molecular weights are low if the amount of initiator applied (1.05 mol % based on monomer) is considered. Low degrees of polymerization (DP) are probably caused by chain-transfer reactions. The polydispersity indices are low if compared to some other radical polymerizations, which may be caused by fractionation during precipitation. After precipitation, polymer yields varied between 20 and 90%.

3.3. Transition Temperatures and Mesophases of SCLCPs. Table 4 summarizes the mesophases of the polymers, their phase transition temperatures and the corresponding entropy changes. The reproducibility of the polymer synthesis was checked by synthesizing two batches of polymer **6-9,0**. Both polymers showed similar molecular weights and transition temperatures (Tables 3 and 4). Because the molecular weights and polydispersity indices of the various polymers are similar direct comparison of transition temperatures appears reasonable. The mesophases in Table 4 were assigned based on the X-ray diffraction patterns of the mesoglass and textures observed with POM. The assignment of mesophases will be discussed later on.

Table 5 represents the X-ray diffraction data, comprising experimental *d* spacings, calculated *d* spacings, the type of the hexagonally ordered mesophase and its correlation length ζ. *d* spacings were determined in the glassy state at room temperature, after the polymer was cooled from the isotropic state to the glassy state at a cooling rate of 5 °C/s. The degree of interdigitation was determined from comparison of experimental *d* spacings in the mesoglass and calculated smectic *d* spacings.

Spacer Length. Figure 2 shows the DSC thermograms of polymers **6-*m*,0**. On heating, the T_g is represented by an endothermic shift in baseline, which can clearly be seen for polymer **6-2,0**. For the other polymers the endothermic peak just after T_g complicates the determination of T_g.

On cooling from the isotropic melt, a sandlike texture was observed with POM that transformed into small domains of bandlike colored textures after annealing for several hours. These bandlike textures, corresponding to an S_A mesophase, became clearer when the cover slip was moved by applying mechanical stress before annealing. Most polymers exhibit an additional transition just above T_g in the DSC thermogram (Figure 2). However, as a result of the high viscosity just above T_g, no change in texture could be observed on passing this transition.

The X-ray data in Table 5 show that polymers **6-*m*,0** exhibit S_{Ad} mesophases. The difference between experimental and calculated *d* spacings increases up to 20% for a spacer length of nine carbon atoms. This increase is comparable to the increase found before for polymers with acrylic backbones.[31] The deviations are ascribed to deviations in the all-trans conformation of the spacer while for the calculated *d* spacings the presence of an all-trans conformation is assumed.

In the wide-angle region of the X-ray diffraction pattern, a sharpening of the reflection corresponding to a *d* spacing of 4.4 Å can be observed; however, this reflection is not resolution limited. This reflection results from hexagonal order within the smectic layers, which disappears just above T_g (Table 4 and Figure 2). Because this reflection is not resolution limited, the correlation length can be calculated from the width at half-height of the reflection (Table 5).

The low values of the correlation length in Table 5 may result from (1) a hexatic smectic B (S_{Bhex}) mesophase (limited positional order and long-range bond-orientational order) or (2) a crystal smectic B (S_{Bcryst}) mesophase (long-range positional and bond-orientational order) in which the correlation length is limited by a finite domain structure. The finite domain structure in the S_{Bcryst} mesophase arises from fluctuations of the hexagonal lattice vector.[32] These fluctuations result in a correlation length of 30−100 Å for SCLCPs with a S_{Bcryst} mesophase.[33] A correlation length of 4−8 Å is found for smectics with liquid packing of the mesogenic groups.[33] According to this description our polymers do not show a S_{Bhex} mesophase. However, on the basis of the presence of enthalpic effects observed with DSC (Figure 2) we denote the mesophase just above T_g as S_{Bhex}. The significance of the different correlation lengths is difficult to estimate because of the

Table 5. Experimental *d* Spacings, Calculated *d* Spacings, Mesophase, and Corresponding Correlation Length ζ Obtained from Wide-Angle X-Ray Diffraction Experiments of Polymers 6-*m*,*p*, 7, and 8 in the Glassy State (at Room Temperature)

polymer	*d* spacings /Å		calcd *d* spacing /Å		mesophase	ζ /Å
			S_A[a]	S_{Ad}[b]		
6-2,0						
6-3,0	22.0; 11.1		19.5	24.1	S_{Bhex}	6.8
6-4,0	23.9; 11.9		20.9	26.6	S_{Bhex}	6.7
6-6,0	26.1; 13.1; 8.75	4.43	23.3	31.8	S_{Bhex}	10.5
6-8,0	30.2; 15.0	4.47	25.7	36.8	S_{Bhex}	9.5
6-9,0	31.8; 15.6	4.44	26.8	39.4	S_{Bhex}	12.5
6-9,2	32.1; 18.0; 16.4; 10.9; 8.17	4.49; 4.08; 3.23	29.5	39.4	S_E	32.0
6-9,3	32.6; 18.4; 16.5; 11.1; 8.34	4.48; 4.09; 3.23	30.5	39.4	S_E	20.0
6-9,5	34.6; 19.0; 17.1; 11.5; 8.61; 5.76	4.42; 4.09; 3.23	33.0	39.4	S_E	15.4
6-9,7	37.2; 20.8; 19.0; 12.7	4.43	35.4	39.4	S_{Bcryst}	42.6
6-9,8	51.9;[c] 38.7; 22.3; 19.8; 13.3	4.43	36.7	61.6;[d] 39.4	S_{Bcryst}	86.2
6-3,8	45.3; 23.5; 15.8		29.1	46.3;[d] 24.1		4.6
6-4,7	45.0; 23.4; 15.8		29.1	47.5;[d] 26.6		4.5
6-6,5	43.0; 32.7; 17.8; 16.5	4.35	29.2	50.1;[d] 31.8	S_{Bhex}	11.1
6-8,3	32.7; 17.8; 16.0; 10.8	4.46; 4.12; 3.25	29.3	36.8	S_E	31.6
7	34.4; 17.6		27.0	39.1		5.8
8						

[a] Calculated based on a smectic layer without interdigitation. [b] Calculated based on an interdigitated mesophase with maximum overlap of the biphenyl moieties (Figure 4). [c] Determined in the S_{Adt} mesophase. [d] Calculated based on an interdigitated mesophase with terminal alkyl group overlap (Figure 8).

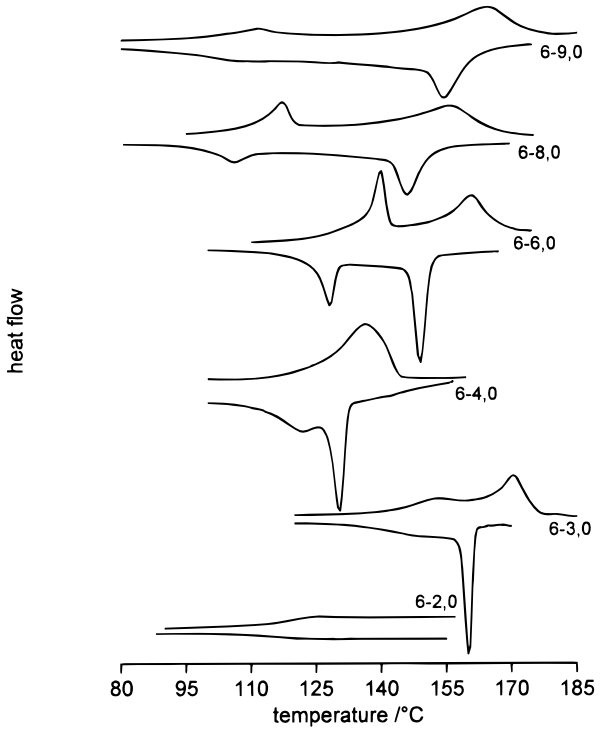

Figure 2. DSC thermograms of polymers **6-*m*,0**. For all compounds the second heating and cooling traces are given.

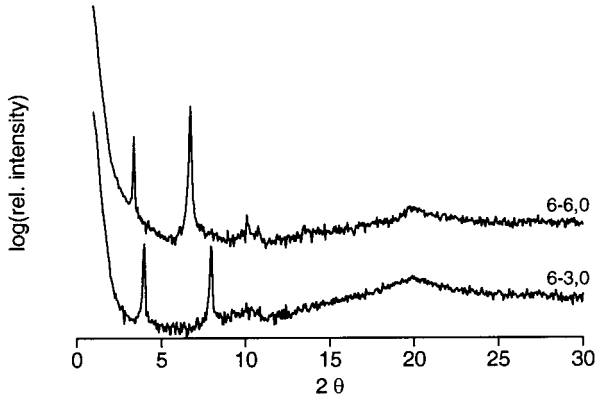

Figure 3. Wide-angle X-ray diffraction patterns of polymer **6-3,0** and **6-6,0** in the glassy state.

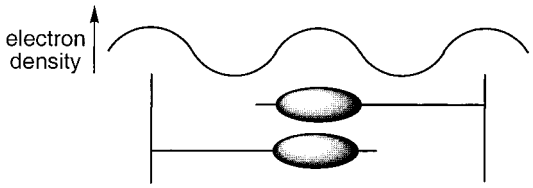

Figure 4. Schematic representation of the ordering of the mesogens and the corresponding electron density profile in an S_{Ad} mesophase.

high cooling rates from the isotropic melt that were used.

Figure 3 shows the X-ray diffraction patterns of polymers **6-3,0** and **6-6,0**. The first-order reflection in the X-ray diffraction pattern of **6-6,0** exhibits a lower intensity than the second order reflection. This results from an additional plane of symmetry in the electron density profile. A model of the probable layer structure (Figure 4) shows that the electron densities are almost equal in both the polymer backbone layer and the mesogen layer. The electron density in the alkyl layer is significantly lower. This additional plane of symmetry induces an apparent *d* spacing (the strongest small angle reflection) which is half the smectic *d* spacing. Because the electron density in the polymer backbone and the mesogen layer are not exactly equal, the first-order reflection can still be observed.

In Figure 3, it can also be seen that the intensity of the second-order reflection as compared to the first-order reflection increases with spacer length. This is thought to result from a more distinct plane of symmetry in the electron density profile for longer spacers: the differences between the maxima in the electron densities of the polymer backbone and the mesogen layer decrease. Furthermore, the electron density fluctuates more strongly in a smectic layer.

The effect of spacer length on the transition temperatures is illustrated in Figure 5. This figure shows that longer spacers broaden the temperature window of the

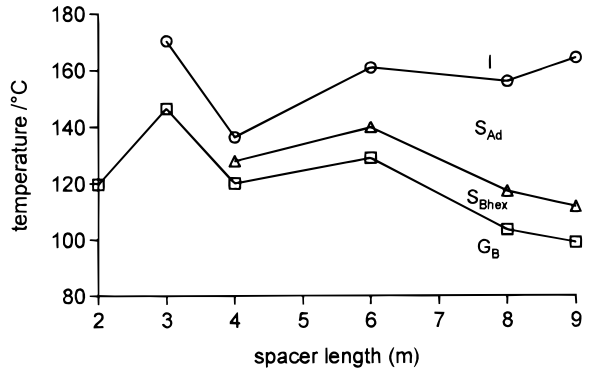

Figure 5. Dependence of the transition temperatures as found with DSC on spacer length *m* for polymers **6-*m*,0**: (□) glass transitions; (△) hexatic smectic B-smectic A_d transitions; (○) isotropic transitions.

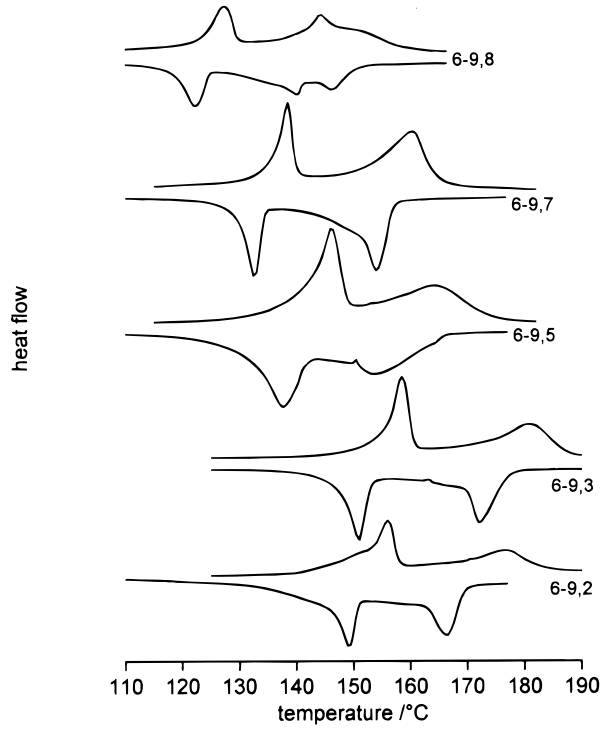

Figure 6. DSC thermograms of polymers **6-9,*p***. For all compounds the second heating and cooling traces are given.

mesophase.[34] The broadening results from both a decrease of T_g and an increase in T_i. The decrease in T_g originates from an increase in distance between backbones which increases the backbone flexibility. The increase in T_i originates from a higher degree of decoupling between the motions of the mesogen and the polymer backbone. On going from a spacer length of three to a spacer length of four carbon atoms, T_g and T_i decreased. This odd behavior has been observed before for SCLCPs with a poly(acrylate) backbone, however, no explanation was given.[35]

Figure 5 also shows a coupling of T_g and the S_{Bhex}–S_{Ad} transition. On cooling, the S_{Ad} mesophase transforms into the more ordered S_{Bhex} mesophase. The hexagonally ordered mesogens restrict the degree of freedom of the polymer backbone to some extent and induce a glass transition temperature. This will be described in more detail in a forthcoming paper.[36]

Terminal Alkyl Group Length. Figure 6 shows the DSC thermograms of polymers **6-9,*p***. From the number of peaks it can be concluded that all polymers except

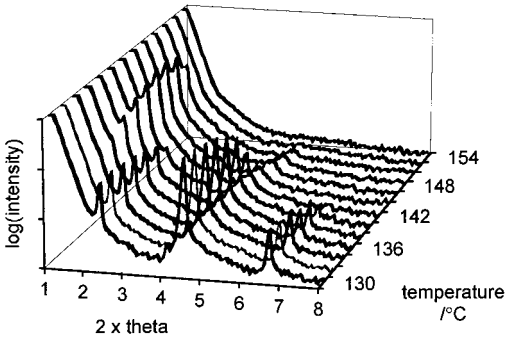

Figure 7. Temperature-dependent wide-angle X-ray diffraction patterns of polymer **6-9,8**.

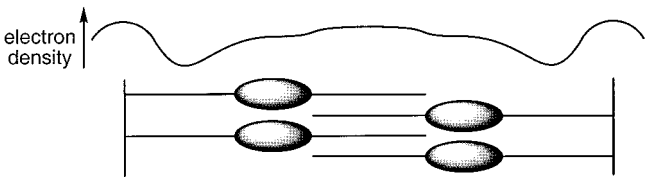

Figure 8. Schematic representation of the ordering of the mesogens and the corresponding electron density profile in an S_{Adt} mesophase.

polymer **6-9,8** show two distinct mesophases. On cooling polymer **6-9,8** shows three peaks which correspond to three distinct mesophases. As for polymers **6-*m*,0**, a hexagonally ordered mesophase is found just above T_g. The peak corresponding to the transition from this mesophase to an S_{Ad} mesophase complicates the exact determination of T_g.

On cooling from the isotropic melt, POM showed that the textures of polymers **6-9,*p*** are comparable to those of polymers **6-*m*,0**. However, polymer **6-9,8** revealed an additional texture. On cooling below 147 °C, small domains with a bandlike texture developed which were surrounded by homeotropic regions. This texture transformed into a sandlike texture upon cooling below 140 °C. The transition temperatures found with POM agreed well with those observed with DSC.

An increase in ordering in smectic layers on going from a methoxy group to longer terminal alkoxy groups results in a higher number of reflections in the X-ray diffraction pattern (Table 5). The experimental *d* spacings agree well with the calculated *d* spacings for an S_{Ad} mesophase, although they are slightly smaller. This difference decreases with increasing terminal alkyl group length because the cavities between mesogens and the neighboring polymer backbones are better filled. As a result the difference in electron density between alkyl layers and biphenyl and backbone layers decreases. This effect is represented by a decrease in the intensity of the second-order reflection as compared to the first-order reflection.

From the DSC thermogram in Figure 6 and POM it can be seen that polymer **6-9,8** exhibits three mesophases. This phenomenon was studied in more detail by temperature-dependent X-ray diffraction experiments (see Figure 7). Between 130 and 144 °C, three reflections can be observed corresponding to an S_{Ad} mesophase. Above 136 °C, a reflection develops corresponding to an interdigitated smectic A mesophase with terminal alkyl group overlap (S_{Adt}), as depicted schematically in Figure 8. A similar mesophase has been reported before.[37] It is assumed that due to interactions between the long terminal alkyl groups and the neigh-

Table 6. Dimensions of the Orthorhombic Cell[a] and the Calculated *d* Spacings of Polymers 6-8,3, 6-9,2, 6-9,3, and 6-9,5 in the Glassy State (G_E)

polmyer	*a*/Å	*b*/Å	*c*/Å
6-8,**3**	8.24	5.30	32.7
6-9,**2**	8.15	5.37	32.1
6-9,**3**	8.17	5.35	32.7
6-9,**5**	8.18	5.25	34.2

[a] Derived from the experimental *d* spacings according to least-squares analysis.

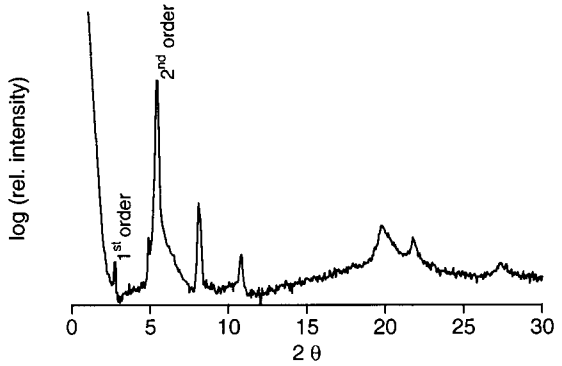

Figure 9. Wide-angle X-ray diffraction pattern of polymer **6-9**,**2**.

boring polymer backbone the S_{Ad} mesophase is destabilized and transforms into an S_{Adt} mesophase at a certain temperature.

The terminal alkyl group length strongly affects the type and degree of hexagonal packing just above T_g. The hexagonally ordered mesophase with the lowest degree of order is observed for polymer **6-9**,**0**. From the small correlation length and the presence of one reflection in the wide-angle region it can be concluded that the mesophase is an S_{Bhex} mesophase. Increasing the terminal alkyl group length results in three reflections in the wide-angle region which correspond to (110), (200) and (210) reflections. This means that polymers **6-9**,**2**, **6-9**,**3** and **6-9**,**5** exhibit a smectic E (S_E) mesophase. The corresponding orthorhombic cell parameters are given in Table 6. From this Table it is clear that terminal alkyl group length does not affect the a and b dimensions of the orthorhombic cell. For longer terminal alkyl groups (polymer **6-9**,**7** and **6-9**,**8**) the (110) and (200) reflections coincide as a result of hexagonal symmetry. The high correlation lengths indicate that the hexagonally ordered mesophase now is a crystal smectic B (S_{Bcryst}) mesophase.[33] The transition from an orthorhombic ordered S_E into a hexagonally ordered S_{Bcryst} mesophase is caused by the long terminal alkyl groups which loosen the mesogen packing.

Figure 9 displays the X-ray diffraction pattern of polymer **6-9**,**5** in the glassy state. The second-order reflection of polymers **6-9**,***p*** has a higher intensity than the first-order reflection, which can be ascribed to an additional plane of symmetry in the electron density profile as was found polymers **6-*m***,**0**. If m > p, polymers **6-9**,***p*** exhibit an additional peak at the low angle side of the second-order reflection ($2\theta \sim 5°$) in the X-ray diffraction pattern. The intensity of this additional peak decreases with terminal alkyl group length. We cannot explain the presence of this additional peak but we assume that a superstructure is superposed on the S_{Ad} mesophase.

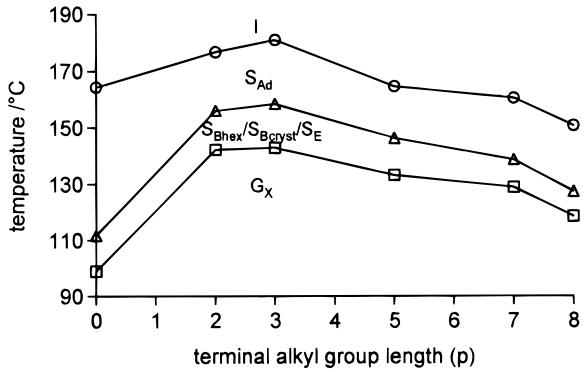

Figure 10. Dependence of the transition temperatures as found with DSC on terminal alkyl group length p for polymers **6-9**,***p***: (□) glass transitions; (△) hexagonally ordered mesophase-smectic Ad transitions; (○) isotropic transitions. Hexagonally ordered mesophases are: hexatic smectic B, crystal smectic B or smectic E.

The effect of terminal alkyl group length on the transition temperatures is illustrated in Figure 10. The mesophase width remains almost constant as a function of terminal alkyl group length but the transition temperatures exhibit a maximum for the polymers with an S_E mesophase ($p = 2, 3, 5$). Transition temperatures decrease if the terminal alkyl group increases from six to nine carbon atoms. A similar trend has been observed before for other LCPs with rigid backbones such as poly(styrene)s[38] and poly(methacrylate)s.[39] In these cases, the backbone restricts the mobility of the mesogens to some extent by preventing them to orient in an appropriate fashion. Long terminal alkyl groups have a plasticizing effect by loosening the mesogen packing. Polymers with flexible backbones, including poly(ethylene oxide)s[40] and poly(carbonate)s,[41] show opposite behavior: longer terminal alkyl groups tend to stabilize the mesogen packing. The observed coupling between T_g and the $S_{Bhex}/S_E/S_{Bcryst}-S_{Ad}$ transition is comparable to the behavior of polymers **6-*m***,***p***.

Table 4 shows that for polymers **6-9**,***p*** the entropy change at T_i slightly increases with increasing terminal alkyl group length. The entropy change at the $H_B/S_E/S_B-S_{Ad}$ transition passes through a maximum for polymers with an S_E mesophase.

Location of the Mesogen in the Side Chain. Figure 11 shows the DSC thermograms of polymers in which the location of the mesogen in the side chain is varied. Polymer **6-8**,**3** exhibits an S_E and an S_{Ad} mesophase (Table 5). Table 6 shows that the dimensions of the orthorhombic cell are comparable to those of polymers **6-9**,***p***.

Polymer **6-6**,**5** shows only one mesophase (Figure 11); however, from the observed *d* spacings in the X-ray diffraction pattern (Table 5) it can be concluded that this polymer exhibits both an S_{Ad} and an S_{Adt} mesophase. This suggest that the S_{Ad} and S_{Adt} mesophases coexist in the temperature range between T_g and T_i and reflects the polydisperse nature of the polymeric material.[42]

The DSC results (Figure 11) and the X-ray reflection results (Table 5) of polymers **6-4**,**7** and **6-3**,**8** show that these polymers exhibit an S_{Adt} mesophase; i.e., the terminal alkyl groups overlap. The transition temperatures of these two polymers are the highest in this series which indicates that the presence of an additional layer of alkyl chains between two layers of mesogens stabilizes the mesophase. The long terminal alkyl

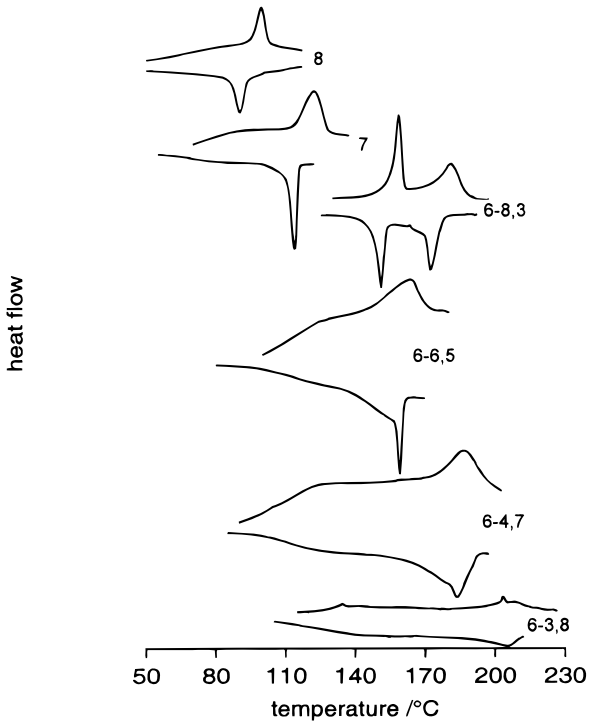

Figure 11. DSC thermograms of polymers **6-*m*,*p*** ($m + p = 11$), **7**, and **8**. For all compounds the second heating and cooling traces are given.

groups fill up the smectic mesophase, especially in the case of short spacer lengths. The short spacers give rise to a low degree of order in the mesophase, which is represented by the low isotropization entropy (Table 4).

Other Structural Variations. From the combination of the DSC results (Figure 11) and the X-ray diffraction results (Table 5) of polymer **7** it follows that this polymer only exhibits an S_{Ad} mesophase. The larger *d* spacing of this S_{Ad} mesophase in comparison to polymer **6-9,0**, the absence of a hexagonally ordered mesophase and the low T_i indicate that the ester linkage partially disturbs the order.

The DSC thermogram of polymer **8** (Figure 11) shows a T_g at 70 °C and a T_i at 99 °C. Between these temperatures POM revealed a vague yellowish texture with bright yellow Maltese crosses around air bubbles. In combination with the absence of reflections in the X-ray diffraction pattern it is concluded that the mesophase is nematic.

4. Conclusions

The alternating copolymerization of maleic anhydride with 1-olefins carrying biphenyl mesogens yields SCLCPs with a low degree of polymerization and high glass transition temperatures. Most of the parent mesogenic 1-olefins did not show liquid-crystalline behavior.

The transition temperatures and degree of order can be altered by molecular structure variations of the SCLCP. Spacer length determines the width of the mesophase: the isotropization temperature increases and the glass transition temperature decreases with increasing spacer length. For long spacers, the terminal alkyl group length has little effect on the mesophase width; however, transition temperatures pass through a maximum for a butoxy terminal group. On cooling from the S_{Ad} into the hexagonally ordered mesophase, the highly ordered mesogens restrict the polymer backbone mobility and induce a glass transition. Different hexagonally ordered mesophases can be observed just above the glass transition temperature depending on the terminal alkyl group length. A methoxy terminal group induces an S_{Bhex} mesophase, intermediate terminal alkyl groups induce an S_E mesophase, and long terminal alkyl groups induce an S_{Bcryst} mesophase.

X-ray diffraction experiments indicate the presence of two different interdigitated smectic A mesophases. If the spacer is longer than the terminal alkyl group, an S_{Ad} mesophase is observed in which the mesogens overlap. If the terminal alkyl group is longer than the spacer, an S_{Adt} mesophase is observed in which the terminal alkyl groups overlap. If spacer and terminal alkyl group length are equal, both mesophases can be observed either in coexistence (**6-6,5**) or in succession (**6-9,8**).

For polymers in which the location of the mesogen in the side chain is altered, it is found that lengthening of the terminal alkyl group and shortening of the spacer leads to the disappearance of the hexagonal order and the appearance of the S_{Adt} mesophase.

Introduction of an ester linkage between the spacer and methoxybiphenyl mesogen lowers the transition temperatures, and no hexagonally ordered mesophase is obtained; however, the S_{Ad} mesophase is still observed. Replacing a methoxy terminal group by a cyano terminal group also lowers transition temperatures, and now only a nematic mesophase is found.

Acknowledgment. We thank the IOP-verf (The Netherlands) for financial support. Mr. C. Padberg (Department of Chemical Technology, University of Twente, The Netherlands) is acknowledged for performing GPC measurements. We are grateful to Dr. E. A. Klop and Mr. R. R. van Puijenbroek (Akzo Nobel Central Research, Arnhem, The Netherlands) for giving us the opportunity to perform X-ray diffraction measurements.

References and Notes

(1) Shibaev, V. P.; Freidzon, Ya. S.; Kostromin, S. G. In *Liquid Crystalline and Mesomorphic Polymers*; Shibaev, V. P., Lam, L., Eds.; Springer-Verlag: New York, 1994.
(2) Finkelmann, H. In *Polymer Liquid Crystals*; Ciferri, A., Krigbaum, W. R., Meyer, R. B., Eds.; Academic Press: New York and London, 1982.
(3) Simmonds, D. J. In *Liquid Crystal Polymers, From Structures to Applications*; Collyer, A. A., Ed.; Elsevier Applied Science: London and New York, 1992.
(4) Percec, V.; Pugh, C. In *Side Chain Liquid Crystal Polymers*; McArdle, C. B., Blackie: Glasgow, U.K., 1989.
(5) Percec, V.; Tomazos, D.; Willingham, R. A. *Polym. Bull.* **1989**, *22*, 199.
(6) Maughon, B. R.; Weck, M.; Mohr, B.; Grubbs, R. H. *Macromolecules* **1997**, *30*, 257.
(7) Stevens, H.; Rehage, G.; Finkelmann, H. *Macromolecules* **1984**, *17*, 851.
(8) Allcock, H. R.; Kim, C. *Macromolecules* **1989**, *22*, 2596.
(9) Percec, V.; Rodriguez-Parada, J. M.; Ericsson, C. *Polym. Bull.* **1987**, *17*, 347.
(10) Laus, M.; Bignozzi, M. C.; Angeloni, A. S.; Galli, G.; Chiellini, E. *Macromolecules* **1993**, *26*, 3999.
(11) Frère, Y.; Yang, F.; Gramain, P.; Guillon, D.; Skoulios, A. *Makromol. Chem.* **1988**, *189*, 419.
(12) Nieuwkerk, A. C.; Marcelis, A. T. M.; Sudhölter, E. J. R. *Macromolecules* **1995**, *28*, 4986.
(13) Komber, H. *Macromol. Chem. Phys.* **1995**, *196*, 669.
(14) Trivedi, B. C.; Culbertson, B. M. In *Maleic Anhydride*; Trivedi, B. C., Ed.; Plenum: New York, 1982.
(15) Schmidt-Naake, G.; Drache, M.; Leonhardt, K. *Macromol. Chem. Phys.* **1998**, *199*, 353.

(16) van der Wielen, M. W. J.; Cohen Stuart, M. A.; de Boer, D. K. G.; Leenaers, A. J. G.; Nieuwhof, R. P.; Marcelis, A. T. M.; Sudhölter, E. J. R. *Langmuir* **1997**, *13*, 4762.
(17) de Boer, D. K. G.; Leenaers, A. J. G.; van der Wielen, M. W. J.; Cohen Stuart, M. A.; Fleer, G. J.; Nieuwhof, R. P.; Marcelis, A. T. M.; Sudhölter, E. J. R. *Physica B* **1998**, *248*, 274.
(18) Frost, A. M.; Kolosentseva, I. A.; Razumovskii, V. V. *Zh. Prikl. Khim.* **1974**, *47*, 731.
(19) Kurbanova, R. A.; Mirzaoglu, R.; Kurbanov, S.; Karatas, I.; Pamuk, V.; Ozcan, E.; Okudan, A.; Güler, E. *J. Adhes. Sci. Technol.* **1997**, *11*, 105.
(20) Bistac, S.; Vallat, M. F.; Schultz, J. *J. Adhes.* **1996**, *56*, 205.
(21) Thery, S.; Jacquet, D.; Mantel, M. *J. Adhes.* **1996**, *56*, 15.
(22) Kolosentseva, I. A.; Frost, A. M.; Razumovskii, V. V. *Zakakras. Mater. Ikh. Primen* **1975**, *2*, 10.
(23) Müller, B.; Mebarek, D. *Angew. Makromol. Chem.* **1994**, *221*, 177.
(24) Vogel, A. I. *Textbook of Practical Organic Chemistry*, 5th ed.; Longman Scientific & Technical: Essex, U.K., 1989; p 886.
(25) Rodriguez-Parada, J. M.; Percec, V. *J. Polym. Sci., Part A: Polym. Chem.* **1986**, *24*, 1363.
(26) Marcelis, A. T. M.; Koudijs, K.; Sudhölter, E. J. R. *Liq. Cryst.* **1995**, *18*, 843.
(27) Hsu, C. S.; Rodriguez-Parada, J. M.; Percec, V. *J. Polym. Sci. Part A: Polym. Chem.* **1987**, *25*, 2425.
(28) Davis, F.; Hodge, P.; Towns, C. R.; Ali-Adib, A. *Macromolecules* **1991**, *24*, 5695.
(29) Rätzsch, M.; Zschoche, S.; Steinert, V.; Schlothauer, K. *Makromol. Chem.* **1986**, *187*, 1669.
(30) Tacx, J. C. J. F.; Meijerink, N. L. J.; Suen, K. *Polymer* **1996**, *37*, 4307.
(31) Ebbut, J.; Richardson, R. M.; Blackmore, J.; McDonnel, D. G.; Verral, M. *Mol. Cryst. Liq. Cryst.* **1995**, *261*, 549.
(32) Davidson, P.; Levelut, A. M. *Liq. Cryst.* **1992**, *11*, 469.
(33) Shibaev, V. P. In *Liquid-Crystal Polymers*; Platé, N. A., Ed.; Plenum Press: New York, 1993.
(34) Nieuwhof, R. P.; Marcelis, A. T. M.; Sudhölter, E. J. R.; van der Wielen, M. W. J.; Cohen Stuart, M. A.; Fleer, G. J. *Macromol. Symp.* **1998**, *127*, 115.
(35) Gemmel, P. A.; Gray, G. W.; Lacey, D.; Alimoglu, A. K.; Ledwith, A. *Polymer* **1985**, *26*, 615.
(36) Wübbenhorst, M.; Nieuwhof, R. P.; Marcelis, A. T. M.; Sudhölter, E. J. R. To be published.
(37) Shibaev, V. P.; Platé, N. A. *Pure Appl. Chem.* **1985**, *57*, 1589.
(38) Niemelä, S.; Selkälä, R.; Sundholm, F.; Taivainen, J. *J. Macromol. Sci.—Pure Appl. Chem.* **1992**, *A29*, 1071.
(39) Kossmehl, G.; Pithart, C. *Acta Polym.* **1991**, *42*, 438.
(40) Reesink, J. B.; Picken, S. J.; Witteveen, A. J.; Mijs, W. J. *Macromol. Chem. Phys.* **1996**, *197*, 1031.
(41) Jansen, J. C. Side-chain liquid crystalline polycarbonates, synthesis, mesomorphic properties and dielectric and mechanical analysis. Thesis Delft University of Technology, The Netherlands, 1996.
(42) Galli, G.; Chiellini, E.; Laus, M.; Caretti, D.; Angeloni, A. S. *Makromol. Chem., Rapid Commun.* **1991**, *12*, 43.

MA981393D